
Gradual Test-Time Adaptation by Self-Training and Style Transfer

Robert A. Marsden*

University of Stuttgart

robert.marsden@iss.uni-stuttgart.de

Mario Döbler*

University of Stuttgart

mario.doebler@iss.uni-stuttgart.de

Bin Yang

University of Stuttgart

bin.yang@iss.uni-stuttgart.de

Abstract

Domain shifts at test-time are inevitable in practice. Test-time adaptation addresses this problem by adapting the model during deployment. Recent work theoretically showed that self-training can be a strong method in the setting of gradual domain shifts. In this work we show the natural connection between gradual domain adaptation and test-time adaptation. We publish a new synthetic dataset called CarlaTTA that allows to explore gradual domain shifts during test-time and evaluate several methods in the area of unsupervised domain adaptation and test-time adaptation. We propose a new method GTTA that is based on self-training and style transfer. GTTA explicitly exploits gradual domain shifts and sets a new standard in this area. We further demonstrate the effectiveness of our method on the continual and gradual CIFAR10C, CIFAR100C, and ImageNet-C benchmark.²

1 Introduction

Deep neural networks achieve remarkable performance under the assumption that training and test data originate from the same distribution. However, when a neural network is deployed in the real world, this assumption is often violated. This effect is known as data shift [1] and leads to a potentially large drop in performance on the test data. While it is possible to improve robustness and generalization during training [2, 3, 4, 5, 6, 7, 8], generalization is limited due to the wide range of potential data shifts [9] that are unknown during training. Instead of trying to generalize to data shifts during training, another area of research follows the idea to adapt the model during test-time. We differentiate between the following research areas: *Unsupervised domain adaptation* (UDA) uses labeled source data and unlabeled target data to train a model with the goal to achieve a high performance on the test data. This is usually done offline, in the sense that first, all available test data are used to optimize the model and then evaluated in a second step. When speaking of online, the performance is directly evaluated after the optimization on a single batch or a single sample in the extreme case. The setting of starting from a pre-trained source model is commonly denoted as *test-time adaptation* (TTA) in the literature. In the case of *fully test-time adaptation* [10], it is further assumed that the source data is not available due to privacy or accessibility issues. Not having access to labeled source data during test-time raises some difficulties. [11] showed that for longer test-time sequences this typically results in error accumulation. One natural way to circumvent error accumulation is to reuse labeled source data during test-time. Even though this can be a limitation, we argue that this is the much more common scenario. Therefore, we address this setting in our work.

*Equal contribution.

²Code is available at: <https://github.com/mariodoebler/test-time-adaptation>

Existing research on TTA focuses on the setting that a model only has to adapt to a single target domain. Needless to say, in practice this setting is very unlikely; it is much more likely that a model encounters different target domains or corruptions without the knowledge when a change occurs. [11] denotes the setting where a model has to adapt at test-time to continually changing target domains (without access to source data) in an online fashion, as *continual test-time adaptation*. Looking at the nature of data shifts in reality, we find that in most cases these shifts do not occur abruptly, but evolve gradually over time. For an autonomous vehicle that has been solely trained on day-time data, it is inevitable that during inference the lighting will vary, due to the changing position of the sun. As a result the performance will drop during test-time. Also shifts due to weather changes or seasonal progression are typical. Other examples mentioned in [12] are evolving road conditions [13], sensor aging [14], or sensor measurement drifts of neural signals received by brain-machine interfaces [15]. We denote this field of gradual shifts during test-time as *gradual test-time adaptation*.

Following the theoretical and empirical analysis of [12] that gradual domain adaptation provides improvements over the traditional approach of direct domain adaptation, we make use of the natural connection between gradual domain adaptation and test-time adaptation. Given a source model and source data, we utilize self-training (ST) to adapt to gradually changing domain shifts during test-time. To further close the domain gaps encountered during test-time, we use a content-preserving style transfer model that is also adapted to new target styles. We suggest that style transfer can be also seen as introducing new gradual domain shifts by creating intermediate domains, benefiting self-training.

Due to the lack of suitable datasets for gradual test-time adaptation, we introduce and publish a new dataset: CarlaTTA. It includes various gradual changes for the field of semantic image segmentation of urban scenes. Our method significantly outperforms recent methods in the area of TTA and one-shot unsupervised domain adaptation. To further demonstrate the effectiveness of our method, we also compare the performance on the continual CIFAR10-to-CIFAR10C, CIFAR100-to-CIFAR100C, and ImageNet-to-ImageNet-C benchmark. We summarize our main contributions as follows:

- We show that our relatively simple method GTTA, which combines self-training and light-weight style transfer, can be very effective by exploiting gradual domain shifts.
- We create and publish a new dataset for urban scene segmentation that enables the exploration of gradual domain shifts in complex scenarios during test-time.
- Adapting the batch normalization (BN) statistics already provides a strong baseline for test-time adaptation [16]. We highlight a variant of adapting BN statistics, which exploits the gradual setting, surpassing existing BN adaptation variants.

2 Related Work

Unsupervised Domain Adaptation (UDA) Since annotating new target data is very time consuming, especially in the area of semantic segmentation [17], there has been a growing interest in mitigating the distributional discrepancy between two domains using unsupervised domain adaptation. Common approaches for UDA try to align either the input space [18, 19, 20, 21, 22], the feature space [23, 24], the output space [25, 26, 27], or several spaces in parallel [22, 21]. One line of work relies on adversarial learning, where a domain classifier tries to discriminate whether some feature maps [28, 18] or output predictions [25, 26, 27] belong to the source or target domain. It is also possible to exploit adversarial learning or adaptive instance normalization (AdaIN) [29] for transferring the target style to source images [18, 22, 20, 19]. Recently, self-training has gained a lot of attraction [30, 31, 32, 33, 34, 23, 24, 35, 21]. ST utilizes a pre-trained (source) model to create predictions for the unlabeled target data. These predictions can then be treated as pseudo-labels to minimize, for example, the cross-entropy. Since high quality pseudo-labels are essential to this approach, most methods differ in how they select or create reliable pseudo-labels.

One-shot Unsupervised Domain Adaptation (OSUDA) As pointed out in [36], even collecting a large amount of unlabeled target data can be very challenging. Therefore, [36] introduced one-shot UDA, where only one single target image is available during the model adaptation. To address this problem, [36] extends the adaptive instance normalization framework of [29] with a variational autoencoder. By selecting styles for which the segmentation model is uncertain, the domain gap is mitigated. Differently, [37] uses a style mixing component within the segmentation model and further adds patch-wise prototypical matching.

Test-time Adaptation (TTA) Although directly generalizing to any test distribution would solve many problems, having absolutely no information about the test environment during training imposes a great challenge. However, during model deployment, one can gain some insight into the test distribution by using the current test batch. This circumstance is also exploited in recent work, where [16] showed that even adapting the batch normalization statistics during test-time can significantly improve the performance on corrupted data. This approach is similar in spirit to [38], which proposes to update the BN statistics for UDA. More sophisticated approaches perform source model optimization during test-time. For example, [10] updates the BN layers by entropy minimization. [39] creates an ensemble prediction through test-time augmentation [40] and then minimizes the entropy with respect to all parameters. Other methods rely on self-supervised learning, using either pre-text tasks to adapt the model [41, 42, 43, 44] or apply contrastive learning [45]. Recent work makes use of diversity regularizers [46, 47] to circumvent collapse to trivial solutions potentially caused by confidence maximization.

Continual Test-time Adaptation Continual test-time adaptation considers online TTA with continually changing target domains. While some of the existing methods can be applied to the continual setting, such as the online version of TENT [10], they are often posed to error accumulation due to miscalibrated predictions [11]. CoTTA [11] uses weight and augmentation-averaged predictions to reduce error accumulation and stochastic restore to circumvent catastrophic forgetting [48].

Gradual Domain Adaptation (GDA) Recent work has indicated that when the domain discrepancy is too large, adapting a model through self-training can be very challenging due to low quality pseudo-labels [12]. This is also true for TTA using self-supervised learning, where a large domain gap can even deteriorate the performance compared to the corresponding source model [42]. Therefore, numerous methods consider the setting of gradual domain adaptation [49, 50, 51], where several intermediate domains exist between source and target. These intermediate domains divide the distribution gap between the source and target domain into several smaller ones [12]. While some of the proposed approaches successively adapt the model using adversarial learning [52, 13], it has been shown that self-training can be very powerful in this setting [12].

3 Gradual Domain Adaptation during Test-Time

Before providing insights into our setting and approach, we first recapitulate the motivation and theory described in [12] for applying self-training in the context of gradually shifting domains.

Preliminaries for gradual domain adaptation GDA splits the potentially large gap between the joint distribution of the source domain P_0 and the target domain P_K into several smaller gaps through a sequence of intermediate domains P_1, P_2, \dots, P_{K-1} . In [12], the gradual shift is further defined as: $\epsilon > 0$, $\rho(P_k, P_{k+1}) < \epsilon$ for all $0 \leq k < K$, where $\rho(P, Q)$ is a function measuring the distance between the distributions P and Q . While the source domain consists of N_0 labeled data samples $S_0 = \{x_i^{(0)}, y_i^{(0)}\}_{i=1}^{N_0}$, there are no labels available for all the other domains $S_k = \{x_i^{(k)}\}_{i=1}^{N_k}$ with $1 \leq k \leq K$. Similar to traditional UDA, all datasets are assumed to be independently sampled from their underlying joint distribution.

Self-training for GDA As described in [12], self-training first utilizes a pre-trained (source) model with parameters θ and output function f_θ to sharpen the model predictions for each unlabeled target sample $\hat{y}_i^{(k)} = \arg \max(f_\theta(x_i^{(k)}))$ into a pseudo-label. Then, ST exploits the pseudo-labels to update the model parameters by minimizing a loss ℓ , which is typically the cross-entropy. The entire procedure can be written as

$$\theta_k = \text{ST}(\theta, S_k) = \arg \min_{\theta \in \Theta} \frac{1}{|S_k|} \sum_{x_i^{(k)} \in S_k} \ell(f_\theta(x_i^{(k)}), \hat{y}_i^{(k)}). \quad (1)$$

Now, if self-training is used for GDA, the formerly mentioned procedure is repeated successively along the sequence of unlabeled domains until the final target domain P_K . For $1 \leq k \leq K$, the whole training process can be written as $\theta_k = \text{ST}(\theta_{k-1}, S_k)$, where θ_0 and θ_K are the parameters of the initial source model and the final target model, respectively.

Theory To derive a bound for the target error, [12] makes four assumptions. For our setting, we want to highlight the following two:

- Separation: for every domain P_k , there exists a linear classifier $\theta_k \in \Theta$ that achieves a low loss of $\mathcal{L}(\theta_k, P_k) \leq \alpha^*$, while being bounded by $\|\theta_k\|_2 \leq R$.
- Gradual shift: Let $\rho(P_k, P_{k+1})$ denote the maximum Wasserstein-infinity distance between two consecutive domains and $\frac{1}{R}$ be the distance from the decision boundary to the data (margin). There exists a ρ such that the maximum per-class distance satisfies $\rho(P_k, P_{k+1}) \leq \rho < \frac{1}{R}$.

Under the four conditions and the derived bound from [12], gradual self-training can obtain zero target error if the number of unlabeled samples is infinite and the initial source model achieves zero error, i.e., $\mathcal{L}(\theta_0, P_0) = 0$. In summary, if the distribution shift ρ is small compared to the margin $\frac{1}{R}$, the model can label most of the samples correctly. Since it is assumed that there exists a model achieving a low margin loss, ST will also learn a model with low margin loss [12].

Inspired by the theory of GDA, we now look at the setting of gradual test-time adaptation. Instead of dealing with fixed intermediate target domains, we simply treat each test batch as a potential intermediate domain. Since we elaborated on the fact that many domain changes in reality are gradual [12], we also assume in general that consecutive batches only contain gradual shifts. Needless to say, this assumption doesn't always hold in practice, which we will address in the next Section 3.1. Given a pre-trained source model trained on labeled source data the model is adapted at test-time on continually and gradually changing domains. At time step t , the model is updated on the current test batch x_t and is directly evaluated on x_t afterwards.

3.1 Methodology

Although the theory showed that self-training is sufficient for small gradual shifts, in practice, not all encountered shifts are gradual in this sense. Therefore, self-training alone is not enough to solve the problem at hand, especially for abrupt and larger shifts [12]. For autonomous driving, such shifts can appear when entering or exiting a tunnel, or if some classes do not occur frequently in an evolving environment. In these cases, additional intermediate domains are required to divide a large gap into smaller ones. We propose to use a content-preserving light-weight style transfer to transfer source images into the encountered target styles. By training on target-like source images in a supervised manner, the decision boundary is moved into the direction of the target domain, resulting in improved pseudo-labels. If the intermediate domain is close to the target domain, self-training will benefit from reliable pseudo-labels further closing the remaining domain gap.

Style Transfer To create the intermediate domains, we leverage a separate style transfer network with parameters θ_D . However, performing style transfer during test-time imposes some challenges. It should be of light weight to guarantee a certain speed and the network should be easily trainable, even with very few test samples. While [53] introduces a method for photo-realistic style transfer during test-time, it is not suitable for our setting since it takes tens of seconds to transfer one single image-pair. This is similar to style transfer based on adversarial learning [54, 55], which can be also unstable during training. Recently, [19] proposed a framework CACE for continual UDA that leverages a VGG19 based style transfer network with two class-conditional adaptive instance normalization (AdaIN) layers [29] to adapt a segmentation model to a sequence of target domains. AdaIN layers [29] re-normalize a content feature map z_i to have the same channel-wise mean and standard deviation as a style feature map z_j :

$$\hat{z}_i = \text{AdaIN}(z_i, z_j) = \sigma(z_j) \frac{z_i - \mu(z_i)}{\sigma(z_i)} + \mu(z_j). \quad (2)$$

The feature maps are extracted by an ImageNet pre-trained and frozen VGG19 encoder. To learn new target styles, only the decoder is updated by minimizing a content and a style loss: $\mathcal{L}_{\theta_D} = \mathcal{L}_c + \lambda_s \mathcal{L}_s$. Clearly, the style transfer operation shown in Eq. 2 will only capture the most predominant style in an image, while missing class-specific differences [19]. Therefore, CACE conditions the re-normalization in Eq. 2 on each class by using class-specific moments. This is accomplished by using the source segmentation mask for the content feature map and the target pseudo-labels for the style feature map. The target moments are stored in style memory Q , allowing to transfer source images into previous styles.

Building our work upon CACE, we pre-train the style transfer network on the source data for a good initialization. For each sample/batch encountered during test-time, we extract and save the corresponding style moments before updating the style network for I_D iterations. In each iteration, we randomly sample a source batch and style moments from the style memory Q and update the parameters of the decoder minimizing the loss \mathcal{L}_{θ_D} .

Subsequently, the task model now exploits the updated style transfer network that provides the intermediate domain by stylizing source images. For I_M iterations the task model minimizes, on the one hand, a cross-entropy loss \mathcal{L}_{CE} for N_s original and transferred source images and, on the other hand, a self-training loss \mathcal{L}_{ST} for the current N_t test samples. The task loss is defined as

$$\mathcal{L}_{\theta_M} = \mathcal{L}_{CE} + \lambda_{ST}\mathcal{L}_{ST} = -\frac{1}{N_s} \sum_{i=1}^{N_s} \sum_{c=1}^C y_{i,c} \log(p_{i,c}) - \lambda_{ST} \frac{1}{N_t} \sum_{i=1}^{N_t} \sum_{c=1}^C \beta_c \hat{y}_{i,c} \log(p_{i,c}), \quad (3)$$

where C is the number of classes, p_i denotes a softmax output, \hat{y}_i represents a sharpened one-hot encoded pseudo-label, and β_c indicates a class-weighting term explained in the next paragraph.

Self-training For successful self-training, reliable pseudo-labels are essential. Recent literature improves the quality through mean-teachers [11, 31, 33], test-time augmentation [39, 11, ?], or other forms of ensembles [21, 24, 34, 56]. Another successful direction is to filter out unreliable predictions [32, 23, 56], sometimes even applying class-conditional thresholds [32, 30]. In general, pseudo-labeling in the context of self-training is prone to error accumulation, since the untrustworthy low confidence predictions have large gradient magnitudes [47]. A simple solution is to only use pseudo-labels corresponding to confident predictions. This is facilitated by the gradual shift assumption, where high confidence can be maintained through self-training.

In particular, we compute \mathcal{L}_{ST} only with pseudo-labels whose softmax probability is at least γ . We refer to the thresholded pseudo-labels as \tilde{y}_i . For the filtered pseudo-labels, we introduce a class-weighting

$$\beta_c = \begin{cases} \frac{\sum_i \tilde{y}_{i,c}}{\sum_i y_{i,c}} & \text{if } \sum_i \tilde{y}_{i,c} \neq 0 \\ 0 & \text{else} \end{cases} \quad (4)$$

that increases the weight for classes where relatively many samples have been removed. The intuition is that if the domain shift increases the uncertainty for a class c , resulting in a large amount of removed pseudo-labels, the model should strongly recapitulate reliable examples of the corresponding class. This is related to diversity regularization, as used in [46, 47], where an additional loss term encourages diverse predictions. A drawback of this approach is that diversity regularization requires to assume the class distribution, which is not available during test-time.

4 Dataset: Gradual Domain Changes for Urban Scene Segmentation

Currently, there are not many datasets that are suited for investigating gradual test-time adaptation. Even though there already exist various real-world and synthetic driving datasets that contain different domains, such as Cityscapes [17], ACDC [57], Waymo [58], BDD100K [59], SYNTHIA [60], and GTA5 [61], they all involve only stationary domains and no sequences with gradual changes. To close this gap we introduce CarlaTTA: a novel dataset that enables the exploration of gradual test-time adaptation for semantic segmentation. We use CARLA [62], an open-source simulator for autonomous driving research, to address various gradual domain shifts. Following the dynamic weather example from CARLA [62], we create five settings that all evolve from the source dataset *clear*, simulating contiguous driving sequences with different domain changes. *day2night* starts with the highest sun altitude (noon) and performs one complete day-night cycle by varying the sun altitude and sun azimuth angle. *clear2fog* addresses cloudiness and fog density, while *clear2rain* varies cloudiness, precipitation, puddles, and wetness. In both settings, the environment parameters are first increased linearly before they again decrease linearly after a short plateau, finally returning to the clear setting. *dynamic* combines the domain changes: *day2night*, *clear2fog*, and *clear2rain*. Not only does it result in overlapping domain shifts, but also introduces new shifts, such as, reflecting lights during a rainy night. To also investigate long-term behavior, *dynamic* contains multiple day-night and weather cycles resulting in a five times longer sequence. *highway* builds on top of the dynamic weather setting. In contrast to the previous datasets which mainly introduce covariate shifts, *highway*



Figure 1: CarlaTTA: A synthetic driving dataset that explores gradual domain shifts in urban scenes.

also introduces label distribution shifts, since the vehicle drives from the city onto the highway. Example images are shown in Figure 1. Further visualizations and insights into our dataset, including a detailed illustration of the weather parameters, are presented in Appendix B.

5 Experiments

5.1 Experiments on CarlaTTA

Setup All approaches are evaluated in the online setting of TTA, where the prediction is evaluated immediately after the encounter of each test batch (a single image in the case of CarlaTTA). We report the mean intersection-over-union (mIoU) over the entire test sequence. All methods use the same pre-trained source model trained for 100k iterations on the source domain *clear*. Following the standard framework in UDA for semantic segmentation [25], we use the DeepLab-V2 [63] architecture with a ResNet-101 as feature extractor. To prevent overfitting to the source domain, we apply random horizontal flipping, Gaussian blur, color jittering, as well as random scaling in the range [0.75, 2] before the image is cropped to a size of 1024×512 . For our method GTTA, the style transfer network is composed of a VGG19-based encoder-decoder architecture, where the encoder weights are pre-trained on ImageNet and frozen afterwards [29].

Implementation details The segmentation model is trained with SGD using a constant learning rate equal to 2.5×10^{-4} , momentum of 0.9, and weight decay of 5×10^{-4} . During test-time adaptation, we use batches consisting of two source samples and two crops of the current test sample generated from the original test size. While one of the source samples is transferred into the current test style, the other is transferred into a previously seen style, which can also be the original source domain. Only pseudo-labels with a minimum confidence of $\gamma = 0.9$ are considered. The self-training loss \mathcal{L}_{ST} is weighted by $\lambda_{ST} = 0.1$ and the model is updated 4 times. The style transfer network is initially trained for 20k iterations using Adam [64] with learning rate 1×10^{-4} and a batch size of 4. During the online adaptation, the style transfer network is updated for 6 iterations for each test batch. Note that we discuss the trade-off between efficiency, which may be important for some applications in test-time adaptation, and performance in Section A.4 of the Appendix.

Baselines Since batch normalization has proven to be very effective during test-time [16], we consider several variations that can be derived from the following equation:

$$\mu_m = (1 - \alpha)\hat{\mu}_m^{(0)} + \alpha\mu_m^{(t)}, \quad \sigma_m = (1 - \alpha)\hat{\sigma}_m^{(0)} + \alpha\sigma_m^{(t)}, \quad (5)$$

where $\hat{\mu}_m^{(0)}$ and $\hat{\sigma}_m^{(0)}$ denote the running mean and standard deviation of channel m , estimated during source training. $\mu_m^{(t)}$ and $\sigma_m^{(t)}$ are the corresponding moments extracted from the current test batch. By using Eq. 5, we can harmonize the notation of BN related baselines: $\alpha = 0$ refers to the commonly known *source* baseline (BN-0), $\alpha = 1$ only exploits the current test statistics (BN-1), and $\alpha = 0.1$

Table 1: mIoU (%) for the different settings of the CarlaTTA dataset. The source model achieves 78.4% mIoU on the *clear* test split.

Method	source-free	day2night	clear2fog	clear2rain	dynamic	highway
BN-0 (source)	✓	58.4	52.8	71.8	46.6	28.7
BN-0.1	✓	62.7	56.5	72.8	52.1	37.2
BN-1	✓	62.0	56.8	71.4	52.6	32.8
BN-EMA	✓	63.4	58.3	73.4	53.9	31.9
TENT-episodic [10]	✓	61.9	56.8	71.4	52.6	32.8
CoTTA [11]	✓	60.2	55.2	69.3	39.6	32.3
ASM [36]	✗	58.5	53.0	69.2	50.2	39.4
SM-PPM [37]	✗	63.1	56.7	72.7	53.7	32.6
GTTA (self-training only)	✗	64.2	50.7	74.8	50.1	23.9
GTTA (style transfer only)	✗	65.0	61.8	74.0	57.5	42.6
GTTA (ours)	✗	68.1	64.5	74.8	58.4	41.4

leverages the source statistics as a prior (BN-0.1). However, none of them exploits gradual domain shifts. Therefore, we further introduce BN-EMA

$$\hat{\mu}_m^{(t)} = (1 - \alpha)\hat{\mu}_m^{(t-1)} + \alpha\mu_m^{(t)}, \quad \hat{\sigma}_m^{(t)} = (1 - \alpha)\hat{\sigma}_m^{(t-1)} + \alpha\sigma_m^{(t)}, \quad (6)$$

which utilizes a combination of the current test batch statistics $(\mu_m^{(t)}, \sigma_m^{(t)})$ and the previous running statistics $(\hat{\mu}_m^{(t-1)}, \hat{\sigma}_m^{(t-1)})$. To further evaluate our method, we compare to several approaches from related fields: TENT [10] uses BN-1 in combination with an entropy minimization strategy with respect to the BN parameters. From OSUDA, we consider ASM [36] and SM-PPM [37]. While ASM uses an AdaIN based style transfer model to explore the style space, SM-PPM integrates style mixing into the segmentation network and combines it with patchwise prototypical matching. Finally, we also evaluate CoTTA [11]. It utilizes BN-1 and a mean teacher with test-time augmentation to perform entropy minimization. Further it introduces stochastic restore, where source pre-trained weights are restored with a certain probability.

5.1.1 Results for CarlaTTA

Our main results are summarized in Table 1. As expected, BN-0 (source) performs the worst by a large margin. However, there are also differences within the BN approaches, which exploit the test statistics. While BN-EMA outperforms for the scenarios where only lighting or weather conditions change, BN-0.1 is absolutely 4.4% better than the second best (BN-1) on the *highway* split. We also conduct experiments using TENT [10], where we found that the episodic setting using small learning rates works best. Nevertheless, TENT could not surpass BN-1. Following [37], we evaluate ASM without the attention module and use 4 updates per test sample. For SM-PPM, we got the best results using 8 adaptation steps. SM-PPM performs better than TENT or ASM, however, it is still slightly worse on average compared to BN-EMA. CoTTA does not perform better than BN-1 and performance significantly drops for the longer *dynamic* sequence. We attribute this to the circumstances that the test sequence is highly correlated and the mean teacher always lags behind the current test domain.

In contrast, our approach using self-training and style transfer substantially outperforms all baselines by a large margin. Compared to the non-adapted source only model, the performance increases by more than 10% in terms of mIoU in most cases. While self-training alone only provides a clear advantage in two out of five cases, it cannot effectively exploit the gradual domain shift in this setting and even suffers from error accumulation. Style transfer, on the other hand, has a clear advantage in all evaluation settings. Since it trains only with labeled source images, it also does not suffer from error accumulation. The combination of both methods now vastly increases the performance on *day2night* and *clear2fog* as through the intermediate domain introduced by style transfer, self-training benefits from more reliable pseudo-labels.

5.1.2 Ablation Studies for CarlaTTA

Denoting Δt as a proxy for the gradual shift, we generate a dynamic sequence which allows to further study the benefits of gradual TTA. By sub-sampling the sequence, we achieve varying degrees of gradual shift. For comparison, we evaluate on the least common multiple. As shown in Table 2 we

further benefit from a smaller delta ($\Delta t/2$), gaining another 1.1%. Increasing the delta leads to a reduced performance, indicating that exploiting gradual shifts is indeed beneficial for our self-training setup. For very small shifts ($\Delta t/4$) we can see a degradation in performance. We hypothesize that too small domain shifts lead to strongly correlated data resulting in a bad optimization. A more detailed ablation study is discussed in Appendix A.2.

Table 2: Investigation of the amount of gradual shift. Δt corresponds to the delta time used for all our standard sequences. The mIoU (%) is reported for the least common multiple. For comparison, BN-0 and BN-1 achieve 39.4 and 49.1, respectively.

	$4\Delta t$	$2\Delta t$	Δt	$\Delta t/2$	$\Delta t/4$
BN-EMA	47.2	48.4	49.5	50.0	50.0
GTTA (ours)	53.3	54.6	55.9	57.0	54.8

5.2 Experiments on CIFAR10C and CIFAR100C

To further demonstrate the effectiveness of our method for test-time adaptation, we evaluate our approach on the commonly used CIFAR10/100C dataset. To investigate the behavior of our method for abrupt shifts, we first consider the continual CIFAR10/100-to-CIFAR10/100C benchmark. Second, we study a gradual CIFAR10/100-to-CIFAR10/100C benchmark, supporting our insights into the benefits of exploiting gradual shifts. Note: Experiments on ImageNet-C are located in Appendix A.3.

CIFAR10C and CIFAR100C CIFAR10C and CIFAR100C were originally published to benchmark robustness of neural networks [65]. The benchmark comprises of 15 corruptions with 5 severity levels, which were applied on the 10,000 test images of the CIFAR10 and CIFAR100 datasets [40], respectively. Following the RobustBench benchmark [66], a pre-trained WideResNet-28 [67] is used for CIFAR10-to-CIFAR10C, and a pre-trained ResNeXt-29 [68] for CIFAR100-to-CIFAR100C. We follow the implementation of [11], which is based on [10]. We use the same setup as for CarlaTTA, but omit the style transfer, only exploiting original source samples. Following [11] a batch size of 200 is used for all experiments. We use Adam [64] as an optimizer with a learning rate of 1e-5.

Continual CIFAR10/100C benchmark We first consider the continual CIFAR10C and CIFAR100C benchmark, as proposed in [11]. Starting with a network pre-trained on the non-corrupted CIFAR10 and CIFAR100 dataset, respectively, the model adapts during test-time to the corrupted images in an online fashion. Unlike in the standard setting, where the pre-trained model is adapted to each corruption type separately, the continual setting measures the test-time performance over a sequence of all corruptions without any knowledge about the current domain. Test-time adaptation is performed under the highest corruption severity level 5.

We compare our method to the source performance (BN-0), all aforementioned BN adaptation variants, TENT-continual [10], which is TENT in the non-episodic setup, and CoTTA [11]. Results are reported in Table 6. Simply evaluating the pre-trained source model results in an average error of 43.5% for CIFAR10C and 46.4% for CIFAR100C. Using the test batch to update the batch statistics (BN-1) already drastically decreases the error, resulting in an average error of 20.4% for CIFAR10C and 35.4% for CIFAR100C. As already pointed out by [11], TENT-continual outperforms BN-1 in early stages, but quickly deteriorates after a few corruptions. This specifically becomes evident for CIFAR100C, where TENT achieves an error of 90.4% for the last corruption. The average performance is still comparable to BN-1 for CIFAR10C, but is significantly worse than the source performance for CIFAR100C. To avoid error accumulation, one can use TENT-episodic instead. However, in the episodic setup, knowledge from previous examples cannot be leveraged, resulting in a performance on par with BN-1. CoTTA shows the best performance for CIFAR10C outperforming BN-1 by 4.2%. Even though our method is proposed for the context of gradual domain shifts, GTTA still performs well in the general context of continual test-time adaptation. GTTA significantly outperforms the previous state-of-the-art method CoTTA on the more challenging continual CIFAR100C task by further decreasing the average error by 3.1%.

Gradual CIFAR10/100C benchmark To further demonstrate the benefits of exploiting gradual domain shifts, we follow [11] and consider a gradual setup. Instead of considering the sequence from the continual task, where corruptions abruptly change in the highest severity, we now start with

Table 3: Classification error rate (%) for the CIFAR10-to-CIFAR10C and CIFAR100-to-CIFAR100C online continual test-time adaptation task on the highest corruption severity level 5. For CIFAR10C the results are evaluated on WideResNet-28, for CIFAR100C, ResNeXt-29 is used. We report the performance of our method averaged over 5 runs.

Method	Time t															Mean	
	Gaussian	shot	impulse	defocus	glass	motion	zoom	snow	frost	fog	brightness	contrast	elastic_trans	pixelate	jpeg		
CIFAR10C	BN-0 (source)	72.3	65.7	72.9	46.9	54.3	34.8	42.0	25.1	41.3	26.0	9.3	46.7	26.6	58.5	30.3	43.5
	BN-0.1	49.1	44.6	55.5	27.0	44.6	23.1	23.7	20.5	26.2	17.8	8.4	25.5	24.0	40.9	28.7	30.6
	BN-1	28.1	26.1	36.3	12.8	35.3	14.2	12.1	17.3	17.4	15.3	8.4	12.6	23.8	19.7	27.3	20.4
	BN-EMA	31.3	26.1	37.1	26.9	38.3	17.6	12.8	19.0	17.4	18.3	8.4	16.0	26.4	25.3	29.3	23.3
	TENT-cont. [10]	24.8	20.6	28.6	14.4	31.1	16.5	14.1	19.1	18.6	18.6	12.2	20.3	25.7	20.8	24.9	20.7
	CoTTA [11]	24.3	21.3	26.6	11.6	27.6	12.2	10.3	14.8	14.1	12.4	7.5	10.6	18.3	13.4	17.3	16.2
	GTTA (ours)	25.0	20.6	29.6	11.9	31.0	13.1	11.2	15.4	15.0	13.4	8.0	11.1	21.1	16.3	22.4	17.7±0.13
CIFAR100C	BN-0 (source)	73.0	68.0	39.4	29.3	54.1	30.8	28.8	39.5	45.8	50.3	29.5	55.1	37.2	74.7	41.2	46.4
	BN-0.1	51.5	48.2	35.3	26.7	43.8	28.1	25.9	34.8	35.0	42.0	25.3	37.4	24.7	47.6	39.0	37.0
	BN-1	42.1	40.7	42.7	27.6	41.9	29.7	27.9	34.9	35.0	41.5	26.5	30.3	35.7	32.9	41.2	35.4
	BN-EMA	43.5	40.3	42.7	32.1	46.3	30.9	27.6	35.6	34.4	44.2	26.5	32.6	39.4	39.9	41.8	37.2
	TENT-cont. [10]	37.2	35.8	41.7	37.9	51.2	48.3	48.5	58.4	63.7	71.1	70.4	82.3	88.0	88.5	90.4	60.9
	CoTTA [11]	40.1	37.7	39.7	26.9	38.0	27.9	26.4	32.8	31.8	40.3	24.7	26.9	32.5	28.3	33.5	32.5
	GTTA (ours)	38.0	33.8	35.2	25.2	34.6	26.6	24.3	28.9	28.0	33.1	23.3	24.7	28.7	25.2	31.8	29.4±0.05

Table 4: Classification error rate (%) for the gradual CIFAR10-to-CIFAR10C and CIFAR100-to-CIFAR100C benchmark averaged over all 15 corruptions. We separately report the performance averaged over all severity levels (@ level 1–5) and averaged only over the highest severity level 5 (@ level 5).

		BN-0	BN-0.1	BN-1	BN-EMA	TENT-cont.	CoTTA	GTTA (ours)
CIFAR10C	Avg. Error (%) @ level 1–5	24.7	18.1	13.7	13.6	20.4	10.9	11.8
	Avg. Error (%) @ level 5	43.5	30.6	20.4	20.3	25.1	14.2	16.6
CIFAR100C	Avg. Error (%) @ level 1–5	33.6	29.0	29.9	29.7	74.8	26.3	24.7
	Avg. Error (%) @ level 5	46.4	37.0	35.4	35.1	75.9	28.3	25.8

severity level 1 and gradually increase the severity until the highest severity. Before switching to the next corruption type the severity is again gradually decreased to level 1.

We again compare to the same baselines as for the continual benchmark and report the average error in Table 4. We differentiate between the average error over all severities and the average error over the highest severity to make it comparable to the continual setup. The effect that TENT-continual’s performance deteriorates over time, is even more prominent in the gradual setup, since we consider a longer sequence. It is the only method that compared to the continual setup has a worse performance (considering the average error @ level 5). The self-training based methods CoTTA and GTTA both benefit from the gradually changing domains. CoTTA achieves a 2% and 4.2% error decrease for CIFAR10C and CIFAR100C, respectively. Our method again shows the best performance on the CIFAR100C dataset by a considerable margin, reducing its average error @ level 5 to 25.8%.

6 Conclusion

In this work we analyzed whether gradual domain shifts can be exploited effectively by self-training during test-time. This is both supported by experiments for the various gradual changes covered by CarlaTTA and the gradual CIFAR10/100-to-CIFAR10/100C benchmark. Further our experiments showed that for more complex data, style transfer can create intermediate domains resulting in reliable pseudo-labels which benefit self-training. On a new published database CarlaTTA, we outperform existing methods by a large margin. Our proposed method also shows stable results on common continual TTA tasks and even results in state-of-the-art results on CIFAR100-to-CIFAR100C. We are sure that CarlaTTA will give other researchers in the field the opportunity to further investigate the setting of gradual test-time adaptation.

7 Acknowledgments

This publication was created as part of the research project "KI Delta Learning" (project number: 19A19013R) funded by the Federal Ministry for Economic Affairs and Energy (BMWi) on the basis of a decision by the German Bundestag.

References

- [1] J. Quiñero-Candela, M. Sugiyama, A. Schwaighofer, and N. D. Lawrence, *Dataset shift in machine learning*. Mit Press, 2008.
- [2] R. Geirhos, P. Rubisch, C. Michaelis, M. Bethge, F. A. Wichmann, and W. Brendel, "Imagenet-trained cnns are biased towards texture; increasing shape bias improves accuracy and robustness," *arXiv preprint arXiv:1811.12231*, 2018.
- [3] D. Hendrycks, N. Mu, E. D. Cubuk, B. Zoph, J. Gilmer, and B. Lakshminarayanan, "Augmix: A simple data processing method to improve robustness and uncertainty," *arXiv preprint arXiv:1912.02781*, 2019.
- [4] E. Tzeng, J. Hoffman, K. Saenko, and T. Darrell, "Adversarial discriminative domain adaptation," in *Proceedings of the IEEE conference on computer vision and pattern recognition*, 2017, pp. 7167–7176.
- [5] D. Hendrycks, S. Basart, N. Mu, S. Kadavath, F. Wang, E. Dorundo, R. Desai, T. Zhu, S. Parajuli, M. Guo *et al.*, "The many faces of robustness: A critical analysis of out-of-distribution generalization," in *Proceedings of the IEEE/CVF International Conference on Computer Vision*, 2021, pp. 8340–8349.
- [6] K. Muandet, D. Balduzzi, and B. Schölkopf, "Domain generalization via invariant feature representation," in *International Conference on Machine Learning*. PMLR, 2013, pp. 10–18.
- [7] J. Tobin, R. Fong, A. Ray, J. Schneider, W. Zaremba, and P. Abbeel, "Domain randomization for transferring deep neural networks from simulation to the real world," in *2017 IEEE/RSJ international conference on intelligent robots and systems (IROS)*. IEEE, 2017, pp. 23–30.
- [8] J. Tremblay, A. Prakash, D. Acuna, M. Brophy, V. Jampani, C. Anil, T. To, E. Cameracci, S. Boochoon, and S. Birchfield, "Training deep networks with synthetic data: Bridging the reality gap by domain randomization," in *Proceedings of the IEEE conference on computer vision and pattern recognition workshops*, 2018, pp. 969–977.
- [9] E. Mintun, A. Kirillov, and S. Xie, "On interaction between augmentations and corruptions in natural corruption robustness," *Advances in Neural Information Processing Systems*, vol. 34, 2021.
- [10] D. Wang, E. Shelhamer, S. Liu, B. Olshausen, and T. Darrell, "Tent: Fully test-time adaptation by entropy minimization," *arXiv preprint arXiv:2006.10726*, 2020.
- [11] Q. Wang, O. Fink, L. Van Gool, and D. Dai, "Continual test-time domain adaptation," *arXiv preprint arXiv:2203.13591*, 2022.
- [12] A. Kumar, T. Ma, and P. Liang, "Understanding self-training for gradual domain adaptation," in *International Conference on Machine Learning*. PMLR, 2020, pp. 5468–5479.
- [13] A. Bobu, E. Tzeng, J. Hoffman, and T. Darrell, "Adapting to continuously shifting domains," 2018.
- [14] A. Vergara, S. Vembu, T. Ayhan, M. A. Ryan, M. L. Homer, and R. Huerta, "Chemical gas sensor drift compensation using classifier ensembles," *Sensors and Actuators B: Chemical*, vol. 166, pp. 320–329, 2012.
- [15] A. Farshchian, J. A. Gallego, J. P. Cohen, Y. Bengio, L. E. Miller, and S. A. Solla, "Adversarial domain adaptation for stable brain-machine interfaces," *arXiv preprint arXiv:1810.00045*, 2018.
- [16] S. Schneider, E. Rusak, L. Eck, O. Bringmann, W. Brendel, and M. Bethge, "Improving robustness against common corruptions by covariate shift adaptation," *Advances in Neural Information Processing Systems*, vol. 33, pp. 11 539–11 551, 2020.
- [17] M. Cordts, M. Omran, S. Ramos, T. Rehfeld, M. Enzweiler, R. Benenson, U. Franke, S. Roth, and B. Schiele, "The cityscapes dataset for semantic urban scene understanding," in *Proceedings of the IEEE conference on computer vision and pattern recognition*, 2016, pp. 3213–3223.
- [18] J. Hoffman, E. Tzeng, T. Park, J.-Y. Zhu, P. Isola, K. Saenko, A. Efros, and T. Darrell, "Cycada: Cycle-consistent adversarial domain adaptation," in *International conference on machine learning*. PMLR, 2018, pp. 1989–1998.
- [19] R. A. Marsden, M. Döbler, and B. Yang, "Continual unsupervised domain adaptation for semantic segmentation using a class-specific transfer," *arXiv preprint arXiv:2208.06507*, 2022.
- [20] Z. Wu, X. Wang, J. E. Gonzalez, T. Goldstein, and L. S. Davis, "Ace: adapting to changing environments for semantic segmentation," in *Proceedings of the IEEE International Conference on Computer Vision*, 2019, pp. 2121–2130.

- [21] Y. Yang and S. Soatto, “Fda: Fourier domain adaptation for semantic segmentation,” in *Proceedings of the IEEE/CVF Conference on Computer Vision and Pattern Recognition*, 2020, pp. 4085–4095.
- [22] Y. Li, L. Yuan, and N. Vasconcelos, “Bidirectional learning for domain adaptation of semantic segmentation,” in *Proceedings of the IEEE Conference on Computer Vision and Pattern Recognition*, 2019, pp. 6936–6945.
- [23] Q. Zhang, J. Zhang, W. Liu, and D. Tao, “Category anchor-guided unsupervised domain adaptation for semantic segmentation,” in *Advances in Neural Information Processing Systems*, 2019, pp. 435–445.
- [24] R. A. Marsden, A. Bartler, M. Döbler, and B. Yang, “Contrastive learning and self-training for unsupervised domain adaptation in semantic segmentation,” *arXiv preprint arXiv:2105.02001*, 2021.
- [25] Y.-H. Tsai, W.-C. Hung, S. Schuler, K. Sohn, M.-H. Yang, and M. Chandraker, “Learning to adapt structured output space for semantic segmentation,” in *Proceedings of the IEEE Conference on Computer Vision and Pattern Recognition*, 2018, pp. 7472–7481.
- [26] T.-H. Vu, H. Jain, M. Bucher, M. Cord, and P. Pérez, “Advent: Adversarial entropy minimization for domain adaptation in semantic segmentation,” in *Proceedings of the IEEE conference on computer vision and pattern recognition*, 2019, pp. 2517–2526.
- [27] Y.-H. Tsai, K. Sohn, S. Schuler, and M. Chandraker, “Domain adaptation for structured output via discriminative patch representations,” in *Proceedings of the IEEE International Conference on Computer Vision*, 2019, pp. 1456–1465.
- [28] Y. Ganin and V. Lempitsky, “Unsupervised domain adaptation by backpropagation,” in *International conference on machine learning*. PMLR, 2015, pp. 1180–1189.
- [29] X. Huang and S. Belongie, “Arbitrary style transfer in real-time with adaptive instance normalization,” in *Proceedings of the IEEE International Conference on Computer Vision*, 2017, pp. 1501–1510.
- [30] Y. Zou, Z. Yu, B. Vijaya Kumar, and J. Wang, “Unsupervised domain adaptation for semantic segmentation via class-balanced self-training,” in *Proceedings of the European conference on computer vision (ECCV)*, 2018, pp. 289–305.
- [31] W. Tranheden, V. Olsson, J. Pinto, and L. Svensson, “Dacs: Domain adaptation via cross-domain mixed sampling,” in *Proceedings of the IEEE/CVF Winter Conference on Applications of Computer Vision*, 2021, pp. 1379–1389.
- [32] K. Mei, C. Zhu, J. Zou, and S. Zhang, “Instance adaptive self-training for unsupervised domain adaptation,” *arXiv preprint arXiv:2008.12197*, 2020.
- [33] P. Zhang, B. Zhang, T. Zhang, D. Chen, Y. Wang, and F. Wen, “Prototypical pseudo label denoising and target structure learning for domain adaptive semantic segmentation,” in *Proceedings of the IEEE/CVF Conference on Computer Vision and Pattern Recognition*, 2021, pp. 12 414–12 424.
- [34] Z. Zheng and Y. Yang, “Unsupervised scene adaptation with memory regularization in vivo,” *arXiv preprint arXiv:1912.11164*, 2019.
- [35] G. Li, G. Kang, W. Liu, Y. Wei, and Y. Yang, “Content-consistent matching for domain adaptive semantic segmentation,” in *European Conference on Computer Vision*. Springer, 2020, pp. 440–456.
- [36] Y. Luo, P. Liu, T. Guan, J. Yu, and Y. Yang, “Adversarial style mining for one-shot unsupervised domain adaptation,” *Advances in Neural Information Processing Systems*, vol. 33, pp. 20 612–20 623, 2020.
- [37] X. Wu, Z. Wu, Y. Lu, L. Ju, and S. Wang, “Style mixing and patchwise prototypical matching for one-shot unsupervised domain adaptive semantic segmentation,” *arXiv preprint arXiv:2112.04665*, 2021.
- [38] Y. Li, N. Wang, J. Shi, X. Hou, and J. Liu, “Adaptive batch normalization for practical domain adaptation,” *Pattern Recognition*, vol. 80, pp. 109–117, 2018.
- [39] M. Zhang, S. Levine, and C. Finn, “Memo: Test time robustness via adaptation and augmentation,” *arXiv preprint arXiv:2110.09506*, 2021.
- [40] A. Krizhevsky, G. Hinton *et al.*, “Learning multiple layers of features from tiny images,” 2009.
- [41] Y. Sun, X. Wang, Z. Liu, J. Miller, A. Efros, and M. Hardt, “Test-time training with self-supervision for generalization under distribution shifts,” in *International Conference on Machine Learning*. PMLR, 2020, pp. 9229–9248.
- [42] Y. Liu, P. Kothari, B. van Delft, B. Bellot-Gurlet, T. Mordan, and A. Alahi, “Ttt++: When does self-supervised test-time training fail or thrive?” *Advances in Neural Information Processing Systems*, vol. 34, 2021.
- [43] A. Bartler, A. Bühler, F. Wiewel, M. Döbler, and B. Yang, “Mt3: Meta test-time training for self-supervised test-time adaption,” in *International Conference on Artificial Intelligence and Statistics*. PMLR, 2022, pp. 3080–3090.
- [44] A. Bartler, F. Bender, F. Wiewel, and B. Yang, “Ttaps: Test-time adaption by aligning prototypes using self-supervision,” 2022. [Online]. Available: <https://arxiv.org/abs/2205.08731>

- [45] D. Chen, D. Wang, T. Darrell, and S. Ebrahimi, “Contrastive test-time adaptation,” *arXiv preprint arXiv:2204.10377*, 2022.
- [46] J. Liang, D. Hu, and J. Feng, “Do we really need to access the source data? source hypothesis transfer for unsupervised domain adaptation,” in *International Conference on Machine Learning*. PMLR, 2020, pp. 6028–6039.
- [47] C. K. Mummadi, R. Huttmacher, K. Rambach, E. Levinkov, T. Brox, and J. H. Metzen, “Test-time adaptation to distribution shift by confidence maximization and input transformation,” *arXiv preprint arXiv:2106.14999*, 2021.
- [48] M. McCloskey and N. J. Cohen, “Catastrophic interference in connectionist networks: The sequential learning problem,” in *Psychology of learning and motivation*. Elsevier, 1989, vol. 24, pp. 109–165.
- [49] J. Hoffman, T. Darrell, and K. Saenko, “Continuous manifold based adaptation for evolving visual domains,” in *Proceedings of the IEEE Conference on Computer Vision and Pattern Recognition*, 2014, pp. 867–874.
- [50] H.-Y. Chen and W.-L. Chao, “Gradual domain adaptation without indexed intermediate domains,” *Advances in Neural Information Processing Systems*, vol. 34, 2021.
- [51] Y. Zhang, B. Deng, K. Jia, and L. Zhang, “Gradual domain adaptation via self-training of auxiliary models,” *arXiv preprint arXiv:2106.09890*, 2021.
- [52] M. Wulfmeier, A. Bewley, and I. Posner, “Incremental adversarial domain adaptation for continually changing environments,” in *2018 IEEE International conference on robotics and automation (ICRA)*. IEEE, 2018, pp. 4489–4495.
- [53] S. Kim, S. Kim, and S. Kim, “Deep translation prior: Test-time training for photorealistic style transfer,” *arXiv preprint arXiv:2112.06150*, 2021.
- [54] P. Isola, J.-Y. Zhu, T. Zhou, and A. A. Efros, “Image-to-image translation with conditional adversarial networks,” in *Proceedings of the IEEE conference on computer vision and pattern recognition*, 2017, pp. 1125–1134.
- [55] J.-Y. Zhu, T. Park, P. Isola, and A. A. Efros, “Unpaired image-to-image translation using cycle-consistent adversarial networks,” in *Proceedings of the IEEE international conference on computer vision*, 2017, pp. 2223–2232.
- [56] M. Chen, H. Xue, and D. Cai, “Domain adaptation for semantic segmentation with maximum squares loss,” in *Proceedings of the IEEE International Conference on Computer Vision*, 2019, pp. 2090–2099.
- [57] C. Sakaridis, D. Dai, and L. Van Gool, “Acdc: The adverse conditions dataset with correspondences for semantic driving scene understanding,” in *Proceedings of the IEEE/CVF International Conference on Computer Vision*, 2021, pp. 10 765–10 775.
- [58] P. Sun, H. Kretschmar, X. Dotiwalla, A. Chouard, V. Patnaik, P. Tsui, J. Guo, Y. Zhou, Y. Chai, B. Caine *et al.*, “Scalability in perception for autonomous driving: Waymo open dataset,” in *Proceedings of the IEEE/CVF conference on computer vision and pattern recognition*, 2020, pp. 2446–2454.
- [59] F. Yu, H. Chen, X. Wang, W. Xian, Y. Chen, F. Liu, V. Madhavan, and T. Darrell, “Bdd100k: A diverse driving dataset for heterogeneous multitask learning,” in *Proceedings of the IEEE/CVF conference on computer vision and pattern recognition*, 2020, pp. 2636–2645.
- [60] G. Ros, L. Sellart, J. Materzynska, D. Vazquez, and A. M. Lopez, “The synthia dataset: A large collection of synthetic images for semantic segmentation of urban scenes,” in *Proceedings of the IEEE conference on computer vision and pattern recognition*, 2016, pp. 3234–3243.
- [61] S. R. Richter, V. Vineet, S. Roth, and V. Koltun, “Playing for data: Ground truth from computer games,” in *European Conference on Computer Vision (ECCV)*, ser. LNCS, B. Leibe, J. Matas, N. Sebe, and M. Welling, Eds., vol. 9906. Springer International Publishing, 2016, pp. 102–118.
- [62] A. Dosovitskiy, G. Ros, F. Codevilla, A. Lopez, and V. Koltun, “CARLA: An open urban driving simulator,” in *Proceedings of the 1st Annual Conference on Robot Learning*, 2017, pp. 1–16.
- [63] L.-C. Chen, G. Papandreou, I. Kokkinos, K. Murphy, and A. L. Yuille, “Deeplab: Semantic image segmentation with deep convolutional nets, atrous convolution, and fully connected crfs,” *IEEE transactions on pattern analysis and machine intelligence*, vol. 40, no. 4, pp. 834–848, 2017.
- [64] D. P. Kingma and J. Ba, “Adam: A method for stochastic optimization,” *arXiv preprint arXiv:1412.6980*, 2014.
- [65] D. Hendrycks and T. Dietterich, “Benchmarking neural network robustness to common corruptions and perturbations,” *arXiv preprint arXiv:1903.12261*, 2019.
- [66] F. Croce, M. Andriushchenko, V. Sehwag, E. Debenedetti, N. Flammarion, M. Chiang, P. Mittal, and M. Hein, “Robustbench: a standardized adversarial robustness benchmark,” *arXiv preprint arXiv:2010.09670*, 2020.

- [67] S. Zagoruyko and N. Komodakis, “Wide residual networks,” *arXiv preprint arXiv:1605.07146*, 2016.
- [68] S. Xie, R. Girshick, P. Dollár, Z. Tu, and K. He, “Aggregated residual transformations for deep neural networks,” in *Proceedings of the IEEE conference on computer vision and pattern recognition*, 2017, pp. 1492–1500.

A Gradual Test-Time Adaptation

A.1 Implementation Details

An overview of our method is given in Algorithm 1. Hyperparameters used for CIFAR-C, ImageNet-C, and CarlaTTA are summarized in Table 5.

Algorithm 1 GTTA Training Procedure

Require: Pre-trained task model θ_M , ImageNet pre-trained VGG19 encoder

- 1: Initialize moment buffer Q
 - 2: **while** Test-time **do**
 - 3: Create pseudo-labels \hat{y}_t and \tilde{y}_t for current test batch x_t
 - 4: Calculate class-weights β_c using Eq. 4
 - 5: Extract class-wise moments using \tilde{y}_t and save moments in buffer Q
 - 6: **for** I_D iterations **do**
 - 7: Sample source batch
 - 8: Draw moments from Q
 - 9: Calculate style transfer loss \mathcal{L}_{θ_D} and update the parameters of the decoder
 - 10: **end for**
 - 11: **for** I_M iterations **do**
 - 12: Sample source batch
 - 13: Transfer source images using previous and current target styles
 - 14: Forward (transferred) source samples and calculate \mathcal{L}_{CE} from Eq. 3
 - 15: Forward test samples and calculate \mathcal{L}_{ST} from Eq. 3
 - 16: Calculate \mathcal{L}_{θ_M} and update task model parameters θ_M
 - 17: **end for**
 - 18: Evaluate on x_t
 - 19: **end while**
-

Table 5: Hyperparameters used for CIFAR-C, ImageNet-C, and CarlaTTA. *batch size (test)* denotes the number of unique test samples, whereas *batch size (total)* consists of both source and test samples, used for one adaptation step.

	CIFAR-C	ImageNet-C	CarlaTTA
optimizer	Adam	Adam	SGD
learning rate	1e-5	1e-5	2.5e-4
momentum	-	-	0.9
weight decay	-	-	0.0005
batch size (test)	200	64	1
batch size (total)	400	128	4
task updates	I_M	4	4
style updates	I_D	6	6
threshold	γ	0.9	0.9
weight	λ_{ST}	1.0	0.1

A.2 Ablation Studies

A.2.1 Error Accumulation

In general, self-training with unfiltered pseudo-labels is prone to error accumulation, mainly caused by large gradient magnitudes of the untrustworthy low confidence predictions [47]. We further elaborate on circumventing error accumulation by simple pseudo-label filtering and show that in the setting of gradual domain shifts we can rely on high-confidence predictions.

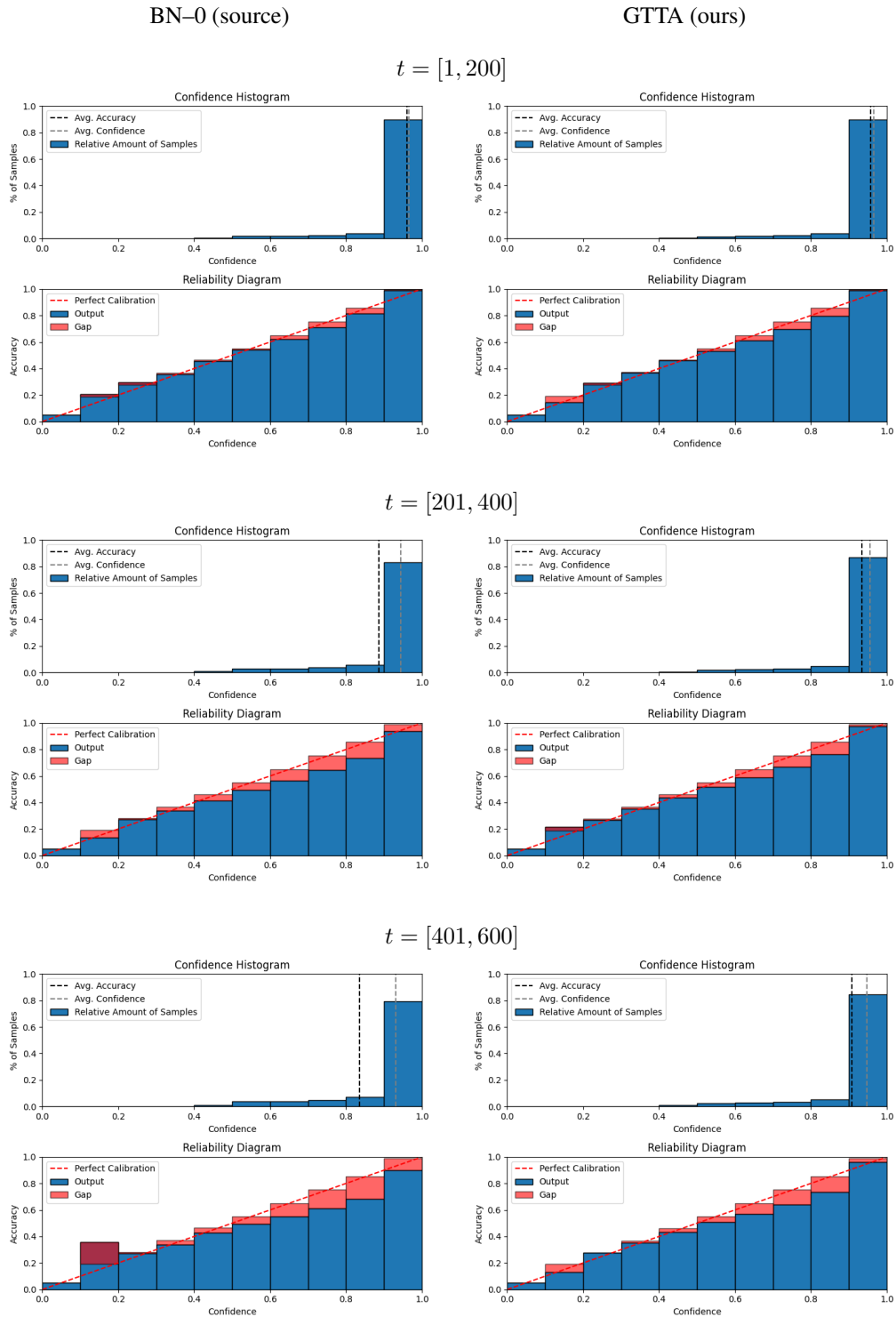


Figure 2: Calibration diagrams for the first half of the *day2night* sequence, where $t = 300$ corresponds to a sun altitude of 0° .

To support our assumption of high confidence predictions in the gradual setup, we visualize calibration diagrams³ for the *day2night* sequence for BN-0 and GTTA in Figure 2. In the beginning of the sequence, where the domain shift is small relative to the source domain, most predictions are of high confidence and accuracy. Predictions with a confidence larger than 0.9 have almost 100% accuracy. With increasing domain shift, the average confidence only slightly decreases. Compared to BN-0, GTTA still achieves high accuracy for high confidence predictions. This becomes even more prominent during night time, which corresponds to the third row of the diagram.

We further look into error accumulation by ablating the usage of source samples, style transfer, and pseudo-label filtering. Starting with pure self-training without any source samples or filtered pseudo-labels, high error accumulation is experienced, resulting in a mIoU of 11.2%. Filtering pseudo-labels alone is not sufficient in preventing error accumulation, improving the performance by just 5.2%. Adding source samples for stabilization boosts the performance, ending up with a mIoU of 64.2%. Transferring source samples into target style further improves the mIoU by 3.9%.

In Table 6, we also study error accumulation for the continual CIFAR100-to-CIFAR100C task. Again, using no additional source samples or not filtering the pseudo-labels results in error accumulation, seen by an increasing error rate over time.

Table 6: Classification error rate (%) of GTTA for the CIFAR100-to-CIFAR100C online continual test-time adaptation task on the highest corruption severity level 5. We ablate the usage of source samples and filtered pseudo-labels.

	Filtered	$t \rightarrow$															Mean
		Gaussian	shot	impulse	defocus	glass	motion	zoom	snow	frost	fog	brightness	contrast	elastic_trans	pixelate	jpeg	
$\lambda_{ST}\mathcal{L}_{ST}$	✗	39.7	37.4	41.1	32.6	44.9	36.4	35.1	41.1	41.0	48.4	37.4	43.4	45.4	42.0	49.7	41.1
$\lambda_{ST}\mathcal{L}_{ST}$	✓	39.2	34.9	38.3	30.5	40.5	33.5	31.7	37.5	37.0	44.1	34.5	39.3	40.3	37.3	44.2	37.5
$\mathcal{L}_{CE} + \lambda_{ST}\mathcal{L}_{ST}$	✗	39.0	35.3	37.3	27.3	37.6	29.0	26.6	31.5	30.6	36.3	26.2	27.6	31.2	27.6	34.3	31.8
$\mathcal{L}_{CE} + \lambda_{ST}\mathcal{L}_{ST}$	✓	38.0	33.8	35.2	25.2	34.6	26.6	24.3	28.9	28.0	33.1	23.3	24.7	28.7	25.2	31.8	29.4

A.2.2 Stability and Sensitivity for CarlaTTA

To investigate the sensitivity of our approach, we conduct several ablation studies on *day2night*. First, averaging the performance of five independent runs, GTTA achieves 68.2 ± 0.06 % mIoU, indicating stable performance. If class-weighting is not used, the performance slightly decreases to 67.3%. A similar observation can be seen when the pseudo-labels are filtered using the strategy from [32], which applies a unique threshold for each class. In this case, the mIoU degrades to 67.6%. Since it is also likely to remain in the source domain during test-time, we conduct an experiment where we evaluate our method on the test split of the *clear* dataset. As shown in Table 7 (a), our method GTTA only slightly deteriorates from BN-0, whereas the performance of BN-1 decreases by nearly 2%. The sensitivity of GTTA with respect to λ_{ST} from Eq. 3 is depicted in Table 7 (b). While smaller values for λ_{ST} have a moderate impact on the performance, the results show a significant drop for $\lambda_{ST} = 0.5$. Last but not least, we study the number of update steps for the task model in Table 7 (c) and the style transfer network in Table 7 (d). As illustrated in (c), the mIoU peaks when the task model is updated four times per test-batch. For the style transfer network, there are only marginal differences considering the number of updates.

Table 7: Mean intersection-over-union on day2night test.

(a)						(b)				
Method	BN-0	BN-0.1	BN-1	BN-EMA	GTTA (ours)	λ_{ST}	0.001	0.01	0.1	0.5
	78.4	78.4	76.6	77.6	78.0		66.1	66.6	68.1	60.9

(c)						(d)					
I_M	1	2	4	6	8	I_D	1	2	4	6	8
	67.6	67.8	68.1	67.9	67.6		68.3	68.3	68.3	68.1	68.0

³<https://github.com/fabiankueppers/calibration-framework>

A.2.3 Non-gradual Shifts

Since we do not have gradual shifts in the real world all the time, we investigate a setting, where the domain changes abruptly from clear to night. Specifically, instead of starting at the first sample of the *day2night* sequence, we begin after 300 samples, corresponding to a sun altitude of 0°. After one complete night-cycle, the sequence reaches its end. We report the results in Table 8. Our method still shows the capability to adapt, reaching a 7.4% higher mIoU than the best BN adaptation approach, namely BN-EMA.

Table 8: Mean intersection-over-union on day2night abrupt.

Method	BN-0	BN-0.1	BN-1	BN-EMA	GTTA (ours)
	43.8	52.8	52.3	54.3	61.7

A.3 ImageNet-C

We further investigate our approach on ImageNet-to-ImageNet-C. We use the same style transfer network with the same (pre-)training strategy as for CarlaTTA. We omit the class-conditioning due to the intuitive reason that corruptions are applied globally and do not have individual effects on the different classes. Using style transfer is in contrast to the CIFAR experiments, where we simply use source images instead of transferred source images. The reason behind this is that for CIFAR we deal with images of size 32×32 , making style transfer impracticable. During test-time we use the same optimizer and learning rate as for the CIFAR experiments. Following [10, 11], we use the standard batch size of 64. We denote that both TENT and CoTTA use different hyperparameters for this setting compared to CIFAR.

Results of the continual ImageNet-to-ImageNet-C benchmark are depicted in Table 9. Our method shows again the best results, achieving an error of 64.8%. To examine the impact of gradual shifts, we also consider the gradual ImageNet-to-ImageNet-C benchmark, presenting the results in Table 10. All self-training based methods show in the gradual setup a better performance (@ level 5) compared to the continual setting, decreasing the error up to 20.7%. To neglect that the performance improvement is not a result of more epochs, we also conduct experiments where we not only iterate once over a corruption type, but five times, before continuing to the next corruption. In this setting performance compared to the continual setting slightly decreases, indicating potential error accumulation.

Table 9: Classification error rate (%) for the ImageNet-to-ImageNet-C online continual test-time adaptation task on the highest corruption severity level 5. ResNet-50 is used as a source model.

Method	Time $t \rightarrow$														Mean	
	<i>Gaussian</i>	<i>shot</i>	<i>impulse</i>	<i>defocus</i>	<i>glass</i>	<i>motion</i>	<i>zoom</i>	<i>snow</i>	<i>frost</i>	<i>fog</i>	<i>brightness</i>	<i>contrast</i>	<i>elastic_trans</i>	<i>pixelate</i>		<i>jpeg</i>
BN-0 (source)	95.3	94.6	95.3	84.9	91.1	86.9	77.2	84.4	79.7	77.3	44.4	95.6	85.2	76.9	66.7	82.4
BN-0.1	89.9	89.2	88.9	80.6	84.8	79.9	70.0	73.4	70.8	62.5	39.1	88.2	67.6	64.8	62.3	74.1
BN-1	87.6	87.5	87.8	87.8	88.0	78.3	64.4	67.6	70.6	54.8	36.4	89.2	58.0	56.4	66.5	72.1
BN-EMA	87.6	87.3	87.3	92.4	88.1	78.8	64.1	69.2	70.2	58.4	37.3	89.2	61.4	58.7	76.2	73.1
TENT-continual	85.8	79.9	78.2	82.1	79.3	71.0	59.3	65.5	66.3	55.3	40.6	80.5	55.6	53.5	59.1	67.5
CoTTA	87.4	85.9	84.5	85.3	83.2	73.3	62.1	63.1	63.7	51.1	38.5	74.4	50.0	44.4	50.0	66.5
GTTA (ours)	82.4	76.5	78.9	83.7	81.9	70.6	59.4	60.2	61.1	48.0	36.7	71.0	52.7	50.9	57.3	64.8

Table 10: Classification error rate (%) for the gradual ImageNet-to-ImageNet-C averaged over all 15 corruptions. We separately report the performance averaged over all severity levels (@ level 1-5) and averaged only over the highest severity level 5 (@ level 5).

	BN-0	BN-0.1	BN-1	BN-EMA	TENT-cont.	CoTTA	GTTA (ours)
Avg. Error (%) @ level 1-5	59.6	52.7	51.4	50.9	52.2	40.8	43.0
Avg. Error (%) @ level 5	82.4	74.1	72.1	71.6	65.3	45.8	56.6

A.4 Trade-off between efficiency and performance

Depending on the application of test-time adaptation, either efficiency or performance can be of higher importance. In Table 11 we highlight the trade-off between efficiency and performance, looking into the number of updates performed for the task network I_M and the number of updates performed for the style transfer network I_D .

Considering the results of GTTA shown in Table 11 (a) and (b), just performing one single update step for the task and style network, still results in a good performance, achieving state-of-the-art for CIFAR100C and the domain shifts introduced by the dataset CarlaTTA. We want to highlight that the current state-of-the-art in continual TTA "CoTTA" requires 32 forward passes due to the application of test-time augmentation and does not scale with increasing the number of updates as shown in Table 11 (c). In this sense our setup with one update step each is much more efficient than CoTTA.

Table 11: (a) mIoU of GTTA for different number of update steps for each domain shift of the CarlaTTA dataset. (b) Average classification error rate (%) of GTTA for different number of update steps. (c) Average classification error rate (%) of CoTTA [11] for different number of update steps.

		(a)				
I_M	I_D	day2night	clear2fog	clear2rain	dynamic	highway
1	1	67.1	60.8	74.6	57.6	44.2
4	6	68.1	64.5	74.8	58.4	41.4

		(b)			(c)			
I_M	I_D	CIFAR10C	CIFAR100C	ImageNetC	I_M	CIFAR10C	CIFAR100C	ImageNetC
1	1	20.1	31.0	67.8	1	16.2	32.5	66.5
4	6	17.7	29.4	64.8	4	17.1	34.6	69.7

B Dataset: CarlaTTA

In the following, we will discuss the specifics about our dataset CarlaTTA. For the generation, CARLA 0.9.13 was used. The data is recorded using an RGB camera and a corresponding semantic segmentation sensor with a resolution of 1920×1024 and a field of view of 40° . Both sensors are positioned 0.5 m forward and 1.2 m upward relative to the ego-vehicle. 14 classes are considered. We visualize the class priors for all sequences in Figure 5.

Table 12: *clear* weather parameters and maximum values used for rain and fog in the settings *clear2rain* and *clear2fog*, respectively.

unit	sun		rain				fog			
	altitude	azimuth	cloudiness	wind	precipitation	deposits	wetness	density	distance	falloff
	$^\circ$	$^\circ$	%	%	%	%	%	%	m	-
clear	90	0	10	5	0	0	0	0	0	0
night (max)	-90	180	-	-	-	-	-	-	-	-
rain (max)	-	-	55	90	80	85	100	-	-	-
fog (max)	-	-	55	90	-	-	10	50	0	0.9

clear The source dataset *clear* is the basis for the four domain changes: *day2night*, *clear2fog*, *clear2rain*, and *dynamic*. The data for *clear* is recorded in Town10HD due to being the only town in CARLA with high resolution textures. To increase diversity we generate multiple sequences using different seeds. Specifically, for each seed, up to 40 vehicles and 20 pedestrians are randomly sampled from all (safe) blueprints. We end up with 3500 train and 500 test samples. *clear* is recorded at noon (sun altitude of 90°) with a cloudiness of 10% and a wind intensity of 5%. All weather parameters are fixed in this setting. The complete overview of the weather parameters used for the *clear* setting is given in Table 12.

day2night, clear2fog, clear2rain, dynamic Different domain changes are introduced by the sequences *day2night*, *clear2fog*, *clear2rain*, and *dynamic*. Each sequence starts with the weather parameters of *clear* and follows the behavior illustrated in Figure 3. The weather model is based on the implementation of CARLA⁴. The maximum values used for the night, rain, and fog setting are depicted in Table 12, with a bar indicating no change from the default parameters of *clear*. While the default sequence length is 1200 samples, *dynamic* contains 6000 samples to have the capability to study long-term behavior. Figure 4 shows every 100th sample of the mentioned domain shifts.

dynamic-slow *dynamic-slow* is only considered for the gradual domain shift ablation study. Compared to the regular *dynamic* sequence, where 1200 samples correspond to one complete day-night cycle, in *dynamic-slow*, 4800 samples correspond to one day-night cycle. This enables the investigation of smaller domain shifts.

highway Since Town10HD does not contain any other settings than urban scenery, we use Town04 for the *highway* sequence. For the corresponding source dataset, we use sequences generated from Town02 (urban setting, similar to Town04) and sequences from Town04 where the ego vehicles only drives in the city. The source dataset contains overall 3000 train and 500 test samples. The *highway* sequence starts in the city of Town04 and shortly after continues on the highway. It follows the same weather behavior as *dynamic*. Examples of the sub-sampled sequence are visualized in the last column in Figure 4.

⁴https://github.com/carla-simulator/carla/blob/0.9.13/PythonAPI/examples/dynamic_weather.py

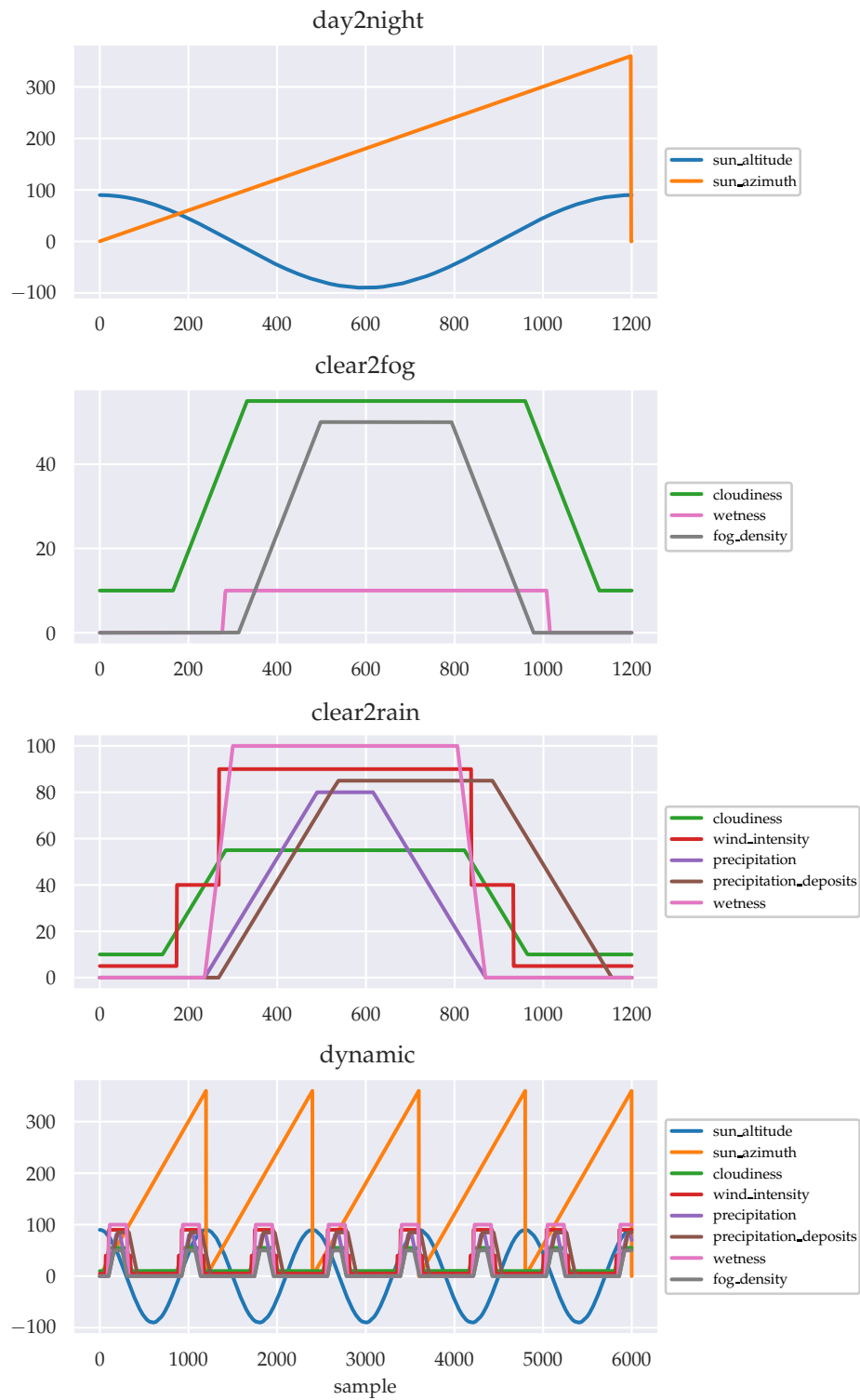


Figure 3: Progression of the weather parameters for the sequences *day2night*, *clear2fog*, *clear2rain*, and *dynamic*. Note that *highway* follows the weather behavior of *dynamic*.

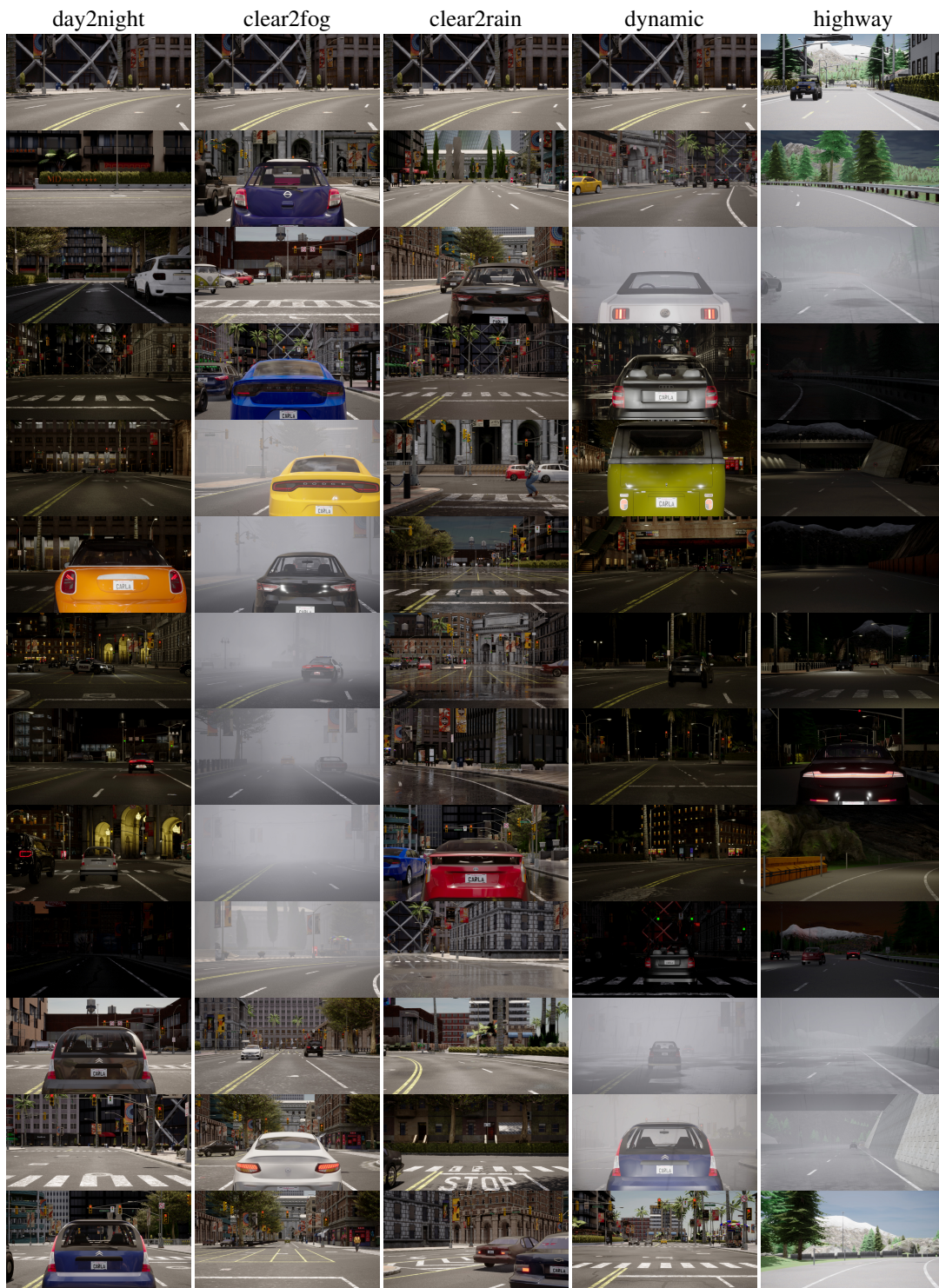


Figure 4: Sequence for the different domain changes. Every 100th example is shown.

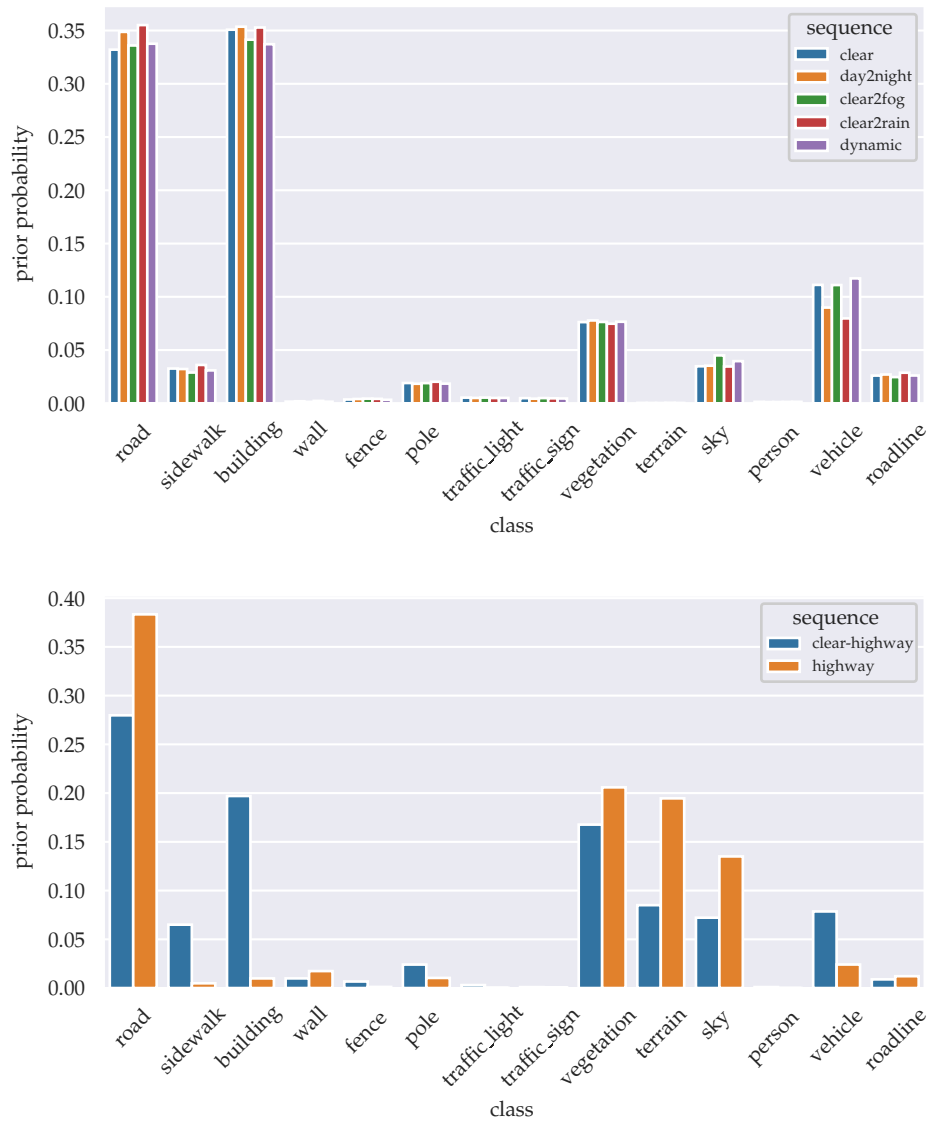


Figure 5: Prior probabilities for the 14 classes. On the top we visualize the prior probabilities corresponding to data originating from Town10HD. On the bottom, we compare *clear-highway* to *highway*. The label distribution shift is clearly prominent as the test-time sequence evolves from an urban scenery into a highway setting.